Indonesian Journal of Environmental Management and Sustainability
e-ISSN:2598-6279 *p*-ISSN:2598-6260

IJEMS

Research Paper

Synthesis and Performance of ZnAl@Layered Double Hydroxide Composites with *Eucheuma cottonii* for Adsorption and Regeneration of Congo Red Dye

Sahrul Wibiyan[1,2], Idha Royani[1], Aldes Lesbani[1,2*]

[1] *Master Program of Materials Science, Graduate School, Universitas Sriwijaya, Palembang, 30662, Indonesia*
[2] *Research Center of Inorganic Materials and Coordination Complexes, Universitas Sriwijaya, Palembang, 30662, Indonesia*
***Corresponding author e-mail**: aldeslesbani@pps.unsri.ac.id

Abstract
This study investigates the synthesis and characterization of ZnAl-layered double hydroxide (ZnAl@LDH) composites modified with *Eucheuma cottonii* (EC) for the adsorption and regeneration of congo red (CR) dye. The ZnAl@LDH was synthesized using a co-precipitation method, and the composite with EC was prepared via hydrothermal techniques. The structural properties of the composites were analyzed using XRD and FTIR. Adsorption experiments were conducted to determine the effects of pH, contact time, concentration, and temperature on dye removal. The adsorption kinetics followed the pseudo-second-order (PSO) model, while the isotherm data best fitted the Freundlich model, indicating multilayer adsorption. The ZnAl@EC composite demonstrated superior adsorption capacity (243.902 mg/g at 40 °C) compared to ZnAl@LDH and EC. Thermodynamic studies revealed that the adsorption process was spontaneous and endothermic for ZnAl@LDH and EC but exothermic for ZnAl@EC. The regeneration study showed that ZnAl@EC retained significant adsorption capacity even after seven cycles, indicating its potential for practical applications in wastewater treatment.

Keywords
Algae, *Eucheuma cottonii*, LDH, Congo Red, Regeneration

Received: 3 June 2024, Accepted: 9 September 2024
https://doi.org/10.26554/ijems.2024.8.3.126-134

1. INTRODUCTION

A serious global environmental issue is the growing problem of water pollution and contamination. This issue is caused by several industrial sectors that release pollutants or waste into sources of water (Basit et al., 2024). The pharmaceutical (Jabeen et al., 2024), fertilizer (Noli et al., 2024), mining (Kang et al., 2023), and textile industries (Sahu and Poler, 2024) are among the various sectors that typically release their waste into rivers or other bodies of water. These industries have the potential to contaminate the environment due to the discharge of effluents containing substances such as ciprofloxacin antibiotic waste (Rohmatullaili et al., 2024), phosphate (Tang et al., 2024), heavy metals (Yao et al., 2024) and congo red dyes (Taher et al., 2021).

Congo red (CR) is an anionic azo dye characterized by a complicated aromatic structure, which can contribute to pollution. The dye exhibits non-biodegradability, high solubility in water, and strong resistance to conventional degradation (Farghali et al., 2022). CR is an anionic azo dye that is based on benzidine. It has an aromatic group that causes significant toxicity, mutagenicity, and carcinogenicity to both aquatic life and humans. It has been claimed that CR undergoes metabolism to form benzidine, which gives it the capacity to accumulate in living organisms and makes it challenging to eliminate from water. Exposure to CR toxicity can result in adverse effects on the neurological system, respiratory system, gastrointestinal system, and mucosal and membrane tissues, leading to symptoms such as nervous system damage, respiratory irritation, diarrhea, vomiting, dizziness, and mucosal and membrane damage. It is crucial to eliminate harmful dyes from water to prevent such injury (Cruz et al., 2023).

Previous techniques employed for dye adsorption included coagulation-flocculation (Goudjil et al., 2021), biodegradation (Eid et al., 2023) and adsorption (Jia and Liu, 2019). However, not all dyes can be efficiently degraded by microorganisms and certain dyes possess non-biodegradable properties. The coagulation-flocculation technique has several limitations that give rise to environmental difficulties, including secondary pollutants, reduced removal effectiveness, and various other limitations (Farghali et al., 2022; Zong et al., 2022). Among all these options, adsorption is the most potent. The selection of adsorption as the preferred method is based on the efficiency, affordability, and

sustainability of adsorbents, which are easily accessible and require simple treatment (Umesh et al., 2024). The option of adsorbent is crucial for achieving efficient dye adsorption.

Layered double hydroxide (LDH) $\left[M^{2+}_{1-x}M^{3+}_{x}(OH)_2\right]^{x+} \cdot A^{m-}_{x/m} \cdot nH_2O$ is a type of inorganic layered material that is highly regarded as an exceptional adsorbent for wastewater treatment. It has a large surface area, allows anions to move easily between layers, is simple to prepare, inexpensive, and non-toxic (Meili et al., 2019). Nevertheless, there is still a need to enhance the stability of LDH in order to ease its recovery and regeneration. In order to address the limitations indicated above, it is necessary to enhance the efficiency of LDH in dye adsorption by modifying it with additional supporting components (Zhang et al., 2024). In our prior study, we enhanced LDH by including *Spirulina platensis* (Sp) (Lesbani et al., 2024), the outcome of this process is the formation of NiAl-Sp and ZnAl-Sp composites, which exhibit adsorption capacities of 478.190 mg/g and 123.457 mg/g, respectively. The utilization of composites made from natural materials, such as algae, has considerable promise and presents a viable method to enhance the effectiveness of LDH as a dye adsorbent and enhance its structural stability. This, in turn, allows for the repeated utilization of LDH-algae composites. Consequently, we performed an experiment to alter LDH by utilizing *Eucheuma cottonii* (EC). We chose to use EC as a material to modify LDH due to the unique properties of carrageenan and polysaccharide compounds found in EC, particularly 3,6-anhydro-D-galactose and D-galactose-4-sulfate. These compounds contribute to EC's high thermal stability (Jumaidin et al., 2017; Majid et al., 2019). By combining EC with LDH, we expect to create a composite material that has a large adsorption capacity, exhibits stable heat resistance and can be reused multiple times.

2. EXPERIMENTAL SECTION

2.1 Chemical and Instrumental

Eucheuma cottonii (EC) obtained from Maluku, Indonesia, aluminum nitrate ($Al(NO_3)_3 \cdot 9H_2O$), zinc nitrate hexahydrate ($Zn(NO_3)_2 \cdot 6H_2O$), congo red ($C_{32}H_{22}N_6Na_2O_6S_2$), sodium hydroxide (NaOH), hydrochloric acid (HCl), and distilled water used in this study were obtained from Merck and used without going through the purification process.

The tools used to analyze material characterization are Rigaku MiniFlex600 x-ray diffractometer and Shimadzu Prestige-21 Fourier Transform Infrared Spectrophotometer. UV-Vis spectrophotometer EMC-18PC-UV was used for analysis in the process of adsorption of congo red dye. The tools used in this research are standard laboratory equipment such as analytical balances, standard glassware such as beakers, measuring cups, drop pipettes, volumetric pipettes, magnetic stirring rods, mortars, ovens, hotplates, filter paper, Buchner funnels and vacuum pumps, shakers, pH meters, and hydrothermal steels.

2.2 EC Preparation

Purified water is used to clean the EC from any remaining contaminants. Next, the EC was dried in an oven at 105 °C to remove any moisture. The EC was pulverized using a mortar and sieved using a 200 mesh sieve.

2.3 ZnAl@LDH Preparation

The synthesis of ZnAl@LDH was achieved by the co-precipitation method, wherein 30 mL of a 0.75 M solution of $Zn(NO_3)_2 \cdot 6H_2O$ was combined with 30 mL of a 0.25 M solution of $Al(NO_3)_3 \cdot 9H_2O$. The resulting mixture was stirred for a duration of 30 minutes. Sodium hydroxide (NaOH) was introduced into the solution until it reached a pH of 8. The mixture was agitated extensively for a duration of 4 hours at a temperature of 80 °C. The mixture was subjected to filtration and subsequently washed with distilled water. Additionally, the resultant product was subjected to desiccation in a 100 °C oven. The ZnAl@LDH was ground into a fine powder using a mortar and pestle, and then filtered through a 200 mesh sieve. X-ray diffraction (XRD) and Fourier transform infrared spectroscopy (FT-IR) were employed to characterize ZnAl@LDH.

2.4 ZnAl@EC Composite Preparation

ZnAl@EC is synthesized using co-precipitation and hydrothermal techniques. The ZnAl@EC synthesis was carried out by reacting 30 mL of a 0.75 M $Zn(NO_3)_2 \cdot 6H_2O$ solution with 30 mL of a 0.25 M $Al(NO_3)_3 \cdot 9H_2O$ solution. Subsequently, the mixture is stirred for a period of 30 minutes. Sodium hydroxide (NaOH) is incrementally introduced into the solution until it reaches a pH value of 8. Subsequently, the mixture is agitated for a period of 15 minutes at a temperature of 80 °C. Afterwards, 3 grams of EC is added to the mixture and stirred using a mechanical mixer for 15 minutes. The solution is introduced into a hydrothermal apparatus and exposed to heating at a temperature of 105 °C for a period of 5 hours. Afterwards, the mixture is filtered and washed with distilled water, and then dried in the oven at a temperature of 100 °C. Afterwards, the ZnAl@EC was polished using a mortar and then filtered through a 200 mesh sieve.

2.5 Adsorption Procedure

The pH_{pzc} was determined by creating a 0.1 M NaCl solution with a volume of 20 mL. The pH of the solution was adjusted within the range of 2-11 using 0.01 M HCl and NaOH. A quantity of 0.02 grams of adsorbent was introduced into the solution, which had been adjusted to the desired pH. The mixture was then subjected to stirring in a shaker for a duration of 12 hours. Various factors such as pH, contact time, concentration, and temperature were manipulated to determine the best conditions for adsorbing congo red dye.

The pH variation process involved the addition of 20 mL of congo red dye solution with a concentration of 50 mg/L. The pH was then altered from 5 to 10 using 0.01 M

NaOH and HCl. The initial absorbance was measured using a UV-Vis spectrophotometer. Subsequently, 0.02 grams of adsorbent was introduced and agitated for a duration of 2 hours. After this, the absorbance of the filtrate was reassessed.

The impact of varying contact time was investigated by introducing 0.02 grams of adsorbent into 20 mL of congo red dye solution. After adsorption, the absorbance was periodically monitored over time intervals ranging from 5 to 210 minutes.

The impact of varying concentration levels was investigated by adding 0.02 grams of adsorbent to 20 mL of dye solution with concentrations of 40, 70, 100, and 130 mg/L. The solution was agitated for the predetermined optimal time, and the absorbance was measured.

The impact of temperature was evaluated by conducting experiments at 30 °C, 40 °C, 50 °C, and 60 °C. The solution was agitated for the predetermined optimal time. The optimal adsorption conditions for dye compounds were identified by measuring absorbance using a UV-Vis spectrophotometer while manipulating the variables of pH, time, concentration, and temperature.

2.6 Reusability Adsorbent

The regeneration process entails placing the adsorbent, which has undergone desorption, into a 20 mL solution containing 100 mg/L of dye. The solution was agitated for a duration of 2 hours, and the residual concentration was measured using a UV-Vis spectrophotometer. The adsorbent was dried and subsequently underwent desorption using an ultrasonic device. The procedure entailed the addition of 25 mL of an aqueous solvent followed by stirring for a duration of 2 hours. Subsequently, the amount of filtrate was measured using a UV-Vis spectrophotometer. The leftover residual substance is thereafter subjected to dehydration and subsequently utilized in the subsequent regeneration cycle.

3. RESULT AND DISCUSSION

3.1 Characterization

The purpose of to evaluate the success of the ZnAl@EC composite synthesis, XRD characterization can be employed to compare the results obtained from the characterization of the raw material and precursor with the results of the composite. The results of XRD analysis of adsorbents can be seen in Figure 1. The LDH displays characteristic diffraction peaks can be seen at Figure 1(b), at specific angles, especially $2\theta = 11.41°$, 23.57°, 34.98°, 39.28°, 46.64°, 60.27°, and 61.63°. These peaks correspond to specific hkl planes, especially (003), (006), (012), (015), (018), (110), and (113), which are typical with ZnAl-LDH (JCPDS No. 48-1022) (Shen et al., 2022). The XRD pattern of EC at Figure 1(a), had two peaks at 16.33° and 22.34°, corresponding to the peaks at (101) and (200) which were determined as type Iβ cellulose (Han et al., 2022; Nissa et al., 2023). Figure 1(c) displays the XRD characterization pattern of the composite, ZnAl@EC, formed by combining EC and ZnAl@LDH. This pattern represents the combined characteristics of both materials, confirming the successful synthesis of the composite.

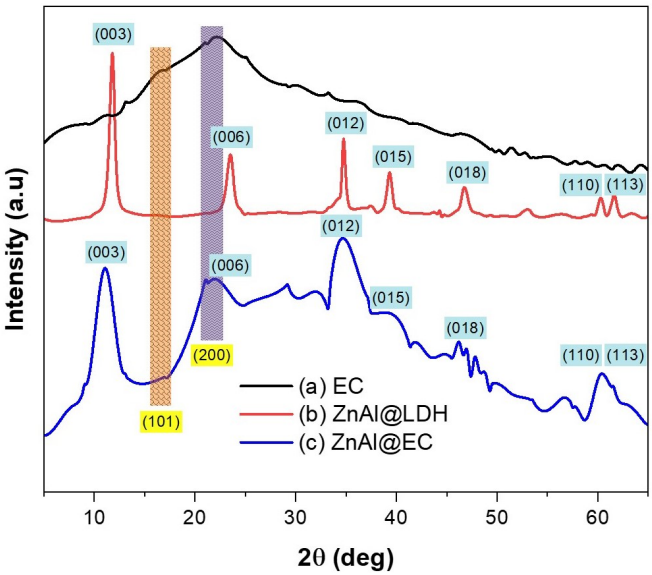

Figure 1. The XRD Patterns of EC (a), ZnAl@LDH (b) and ZnAl@EC (c)

Figure 2 shows the FTIR spectra of the EC, ZnAl@LDH, and ZnAl@EC. Figure 2(a) depicts the FTIR spectrum of EC, which shows the characteristic bands of the functional group of EC. Wide peaks from 3100 to 3600 cm^{-1} were identified as the stretching vibration of hydroxyl groups related to the hydrophilic ability of carrageenan (Firdayanti et al., 2023). The presence of a very strong band at 1243 cm^{-1}, which represents the O=S=O stretching vibrations due to the S=O of the sulfate ester, was observed. In addition, the region around 1081 cm^{-1} was identified as a C-O bond. The signal at 933 cm^{-1} was identified as the C-O-C vibrational mode of the 3,6-anhydro-D-galactose (Yuliarti et al., 2023). The detection of an infrared band at a wavenumber of 841 cm^{-1} indicated the presence of C-O-SO_3 in D-galactose-4-sulphate. The peak at 1544 cm^{-1} signaled the presence of a CH_3 group, the peak at 1632 cm^{-1} was identified as an OH group, and the peak at 1382 cm^{-1} was related to the bending of the CH bond (Li et al., 2018; Tye et al., 2018; Wulandari et al., 2018).

Figure 2(b) shows the FTIR characterization results of ZnAl@LDH at specific peaks of 565 cm^{-1} and 751 cm^{-1}, which are associated with M-O and M-O-M stretching. The peak at 751 cm^{-1} is caused by Zn-O bending, while the peak at 565 cm^{-1} is caused by Al-O bending. The sharp peak at 1381 cm^{-1} is due to the stretching of NO_3 nitrate in the sample, which confirms the presence of layered regions in the ZnAl@LDH structure. The results of the FTIR analysis of ZnAl@EC, identified as having a combined pattern with the

spectra of EC and ZnAl@LDH, concluded that the functional groups of EC were not lost when merging into a composite with ZnAl@LDH Ahmad et al. (2023); Antoniak-Jurak et al. (2021); Tang et al. (2024).

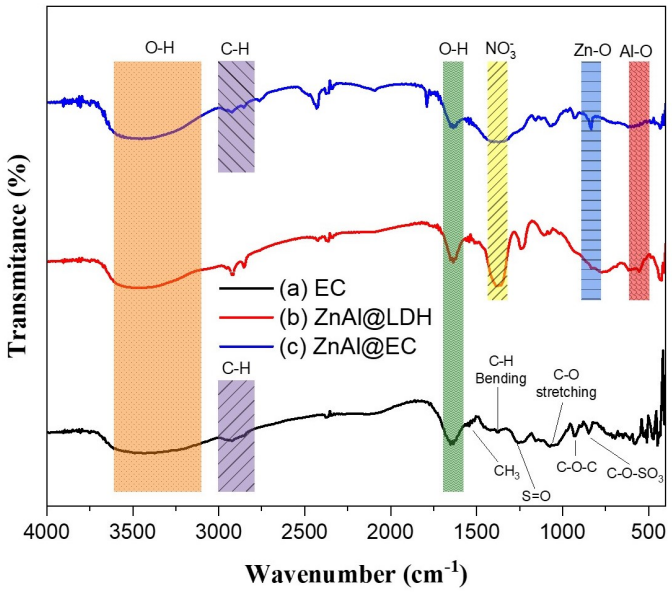

Figure 2. The FTIR spectrum of EC (a), ZnAl@LDH (b) and ZnAl@EC (c)

3.2 Effects of pHpzc and pH of Adsorption

Figure 3 shows the combined graph between pH_{pzc} and the optimum pH variation of congo red dye adsorption. This graph is joined but not connected between the two parameters. The x-axis is the initial pH between the two parameters, while the y-axis is separate pH_{pzc} y-axis ΔpH and adsorption pH variation y-axis adsorbed concentration. The pH_{pzc} of EC, ZnAl@LDH and ZnAl@EC materials were 6.24, 6.60 and 6.77 respectively. ZnAl@LDH which has a brucite interlayer of $Zn(OH)_2$ and $Al(OH)_4$, has a pH_{pzc} of 6.60 This allows for anion exchange interactions, being positively charged below pH 6.60 and negatively charged above also applicable for ZnAl@EC composites (Zhu et al., 2022). EC, ZnAl@LDH and ZnAl@EC materials are all optimum at pH 6 with adsorbed CR dye concentrations of 17.02%, 37.54% and 45.26% respectively. As seen from Figure 3, all materials have optimum CR dye adsorption conditions above pH_{pzc} which indicates the material has a positive charge where adsorption can occur because the adsorbate is anionic (Ravichandran et al., 2023).

3.3 Effects of Adsorption Contact Time

The adsorption graph along with the adsorption kinetics graph of CR dye can be seen in Figure 4. EC, ZnAl@LDH and ZnAl@EC materials had their optimum adsorption time at 55 minutes with adsorbed concentrations of 43.67 mg/L,

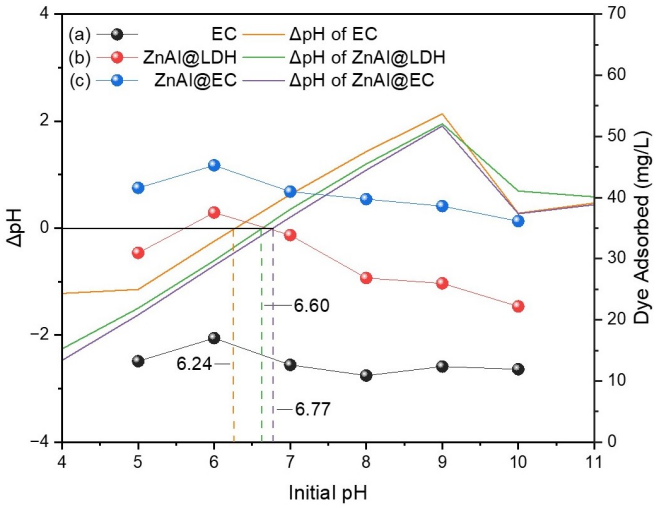

Figure 3. The Graphs of pHpzc and pH Adsorption of EC (a), ZnAl@LDH (b) and ZnAl@EC (c)

58.02 mg/L and 82.31 mg/L respectively. The optimum condition of absorption is reached when absorption has reached equilibrium conditions (Silva et al., 2020). The adsorption kinetics model can be seen in Table 1.

The adsorption kinetics of EC, ZnAl@LDH, and ZnAl@EC adsorbents were analyzed using Pseudo First-Order (PFO) and Pseudo Second-Order (PSO) kinetic models. All adsorbents tended to give a good fit to the PSO kinetic model where the regression values of the three were closest to 1 in this kinetic model. The experimental adsorption capacities (Qe_{exp}) for EC, ZnAl@LDH, and ZnAl@EC were 43.675 mg/g, 58.018 mg/g, and 82.316 mg/g, respectively. The adsorption experimental data fitted better to the calculated adsorption capacity (Qe_{calc}) of the PSO kinetics model with values of 44.843 mg/g, 59.524 mg/g, and 84.034 mg/g, respectively. The PSO adsorption kinetics model explains that the interactions occurring in this adsorption are more likely to be chemical adsorption Haryanto et al. (2017). However, it does not rule out the possibility that adsorption also involves interactions between the adsorbent and adsorbate through physical bonds, as the value of R^2 for the PFO adsorption kinetics is not much different from the PSO model where the value is also close to 1. The rate constants k_1 and k_2 describe the speed of recombination in the adsorption process. The greater the value of the reaction rate constant, the greater the adsorption speed. The rate constants of the three adsorbents EC, ZnAl@LDH, and ZnAl@EC are greater at the k_1 constant value, which can be explained by the faster adsorption process of physical interaction between adsorbent and adsorbate.

Table 1. The Kinetic Parameters PFO and PSO models by EC, ZnAl@LDH and ZnAl@EC

Adsorbent	Qe_{exp} (mg/g)	Pseudo first-order			Pseudo second-order		
		Qe_{calc} (mg/g)	k_1 (min^{-1})	R^2	Qe_{calc} (mg/g)	k_2 (g/mg)/min	R^2
EC	43.675	36.635	0.077	0.9312	44.843	0.005	0.998
ZnAl@LDH	58.018	37.179	0.057	0.8672	59.524	0.006	0.999
ZnAl@EC	82.316	59.580	0.053	0.9094	84.034	0.003	0.999

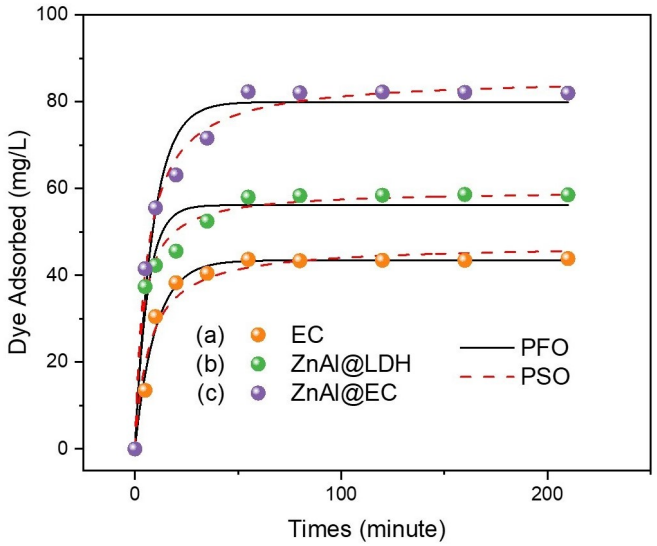

Figure 4. The Impact of Adsorption Contact Time of EC (a), ZnAl@LDH (b) and ZnAl@EC (c)

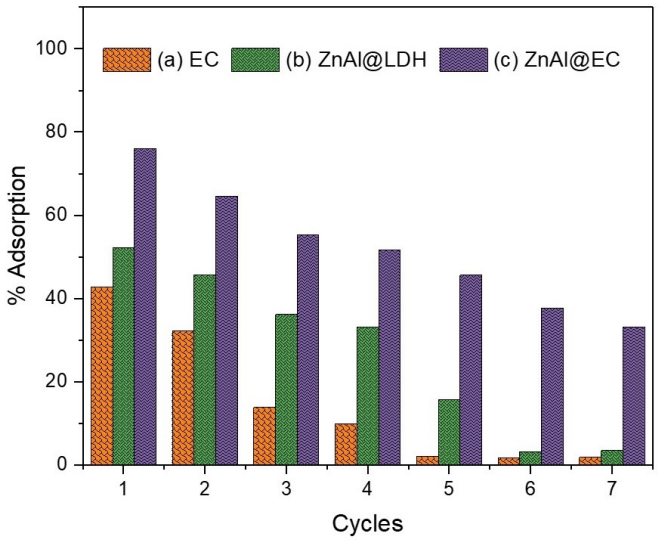

Figure 5. Regeneration Cycle Adsorption of EC (a), ZnAl@LDH (b) and ZnAl@EC (c)

3.4 Effects of Concentration and Temperature on Adsorption

Table 2 shows the adsorption isotherm data of materials EC, ZnAl@LDH, and ZnAl@EC. Materials tend to be more suitable for the Freundlich isotherm model as seen from the R^2 value in the Freundlich isotherm model, which is closer to 1 than in the Langmuir isotherm model. The value of n in EC and ZnAl@LDH materials is $n < 1$ and the value of n in ZnAl@EC is $n > 1$. The value of n indicates the ease of adsorption occurring on the adsorbent. A value of $n < 1$ indicates less favorable adsorption or less ease of occurrence, whereas $n > 1$ indicates that adsorption is favorable or easier to occur. The $Q_{\max}$ values of EC, ZnAl@LDH, and ZnAl@EC materials are 38.023 mg/g at 40 °C, 103.10 mg/g at 30 °C, and 243.902 mg/g at 40 °C, respectively. The adsorption capacity of the materials decreased with increasing temperature, indicating that adsorption is better at lower temperatures.

The adsorption thermodynamic data at Table 3 for EC, ZnAl@LDH, and ZnAl@EC adsorbents at 130 mg/L concentration showed different characteristics related to ΔH, ΔS, and ΔG. For EC adsorbent, the ΔH value of 13.667 kJ/mol indicates that the adsorption process is endothermic, where energy is required for adsorption to occur. The ΔS value of 0.047 kJ/mol indicates an increase in system disorder as adsorption proceeds. Meanwhile, negative ΔG values at various temperatures (303 K to 333 K) indicate that the process is spontaneous, with decreasing spontaneity at higher temperatures. The ZnAl@LDH adsorbent had a ΔH of 10.619 kJ/mol, also indicating endothermic adsorption, but with a lower ΔS value (0.038 kJ/mol), indicating a smaller entropy change compared to EC. The ΔG value for ZnAl@LDH is also negative, indicating the spontaneity of the process which increases with decreasing temperature. In contrast, for ZnAl@EC, ΔH is negative (-10.766 kJ/mol), indicating that the adsorption process is exothermic, where energy is released during the process. The negative ΔS value (-0.027 kJ/mol) indicates a decrease in the disorder of the system, and the ΔG value remaining negative over a wide range of temperatures indicates the spontaneity of the process, although it decreases slightly at higher temperatures.

3.5 Regeneration Study of Adsorbent

The Figure 5. shows the cycle of regeneration for reuse of each materials Regeneration. Data for adsorption of CR dye by various adsorbents showed a significant decrease in

Table 2. The Adsorption Isotherm Langmuir and Freundlich Parameter by EC, ZnAl@LDH and ZnAl-EC

Adsorbent	T (°C)	Langmuir			Freundlich		
		Q_{max}	kL	R^2	n	kF	R^2
EC	30	33.223	0.007	0.844	0.611	29.771	0.953
	40	38.023	0.008	0.847	0.620	21.232	0.940
	50	25.707	0.008	0.853	0.566	54.929	0.950
	60	13.569	0.009	0.734	0.482	288.071	0.972
ZnAl@LDH	30	103.10	0.007	0.956	0.728	3.584	0.999
	40	89.286	0.008	0.897	0.704	4.639	0.996
	50	85.470	0.006	0.938	0.722	5.416	0.999
	60	76.336	0.007	0.918	0.694	6.159	0.993
ZnAl@EC	30	243.902	0.018	0.957	1.301	6.415	0.986
	40	232.558	0.016	0.975	1.320	5.706	0.995
	50	204.082	0.017	0.961	1.381	5.322	0.997
	60	200.000	0.016	0.993	1.371	5.243	0.993

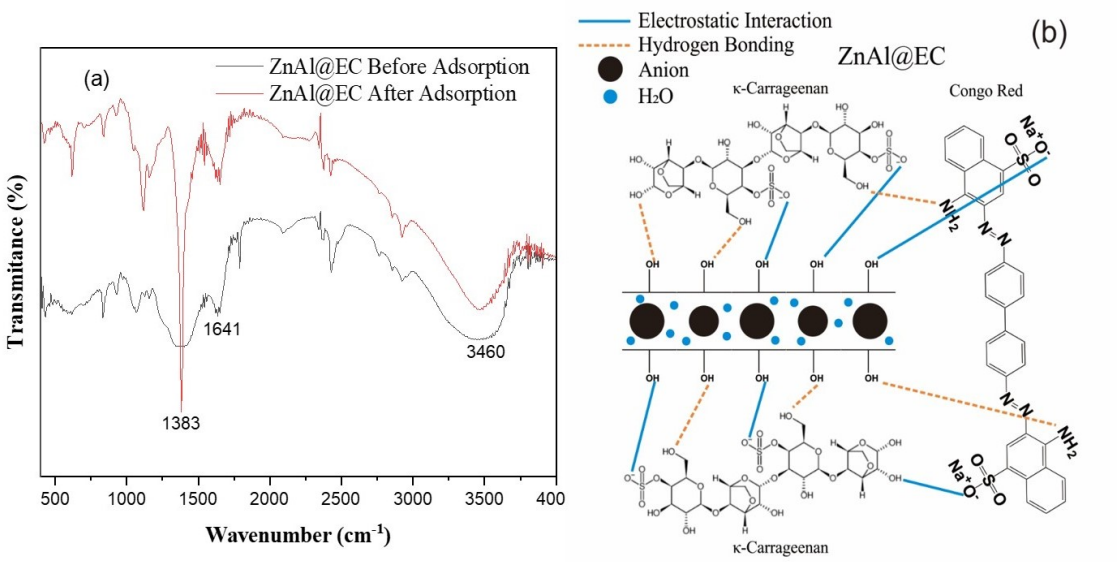

Figure 6. The FTIR Spectrum Before and After Adsorption of ZnAl@EC (a) and Schematic illustration of CR Adsorption Mechanism (b)

Table 3. The Adsorption Thermodynamic Parameter by EC, ZnAl@LDH and ZnAl@EC

Adsorbent	Concentration (mg/L)	ΔH (kJ/mol)	ΔS (kJ/mol)	ΔG (kJ/mol)			
				303 K	313 K	323 K	333 K
EC	130	13.667	0.047	-1.090	-0.634	-1.238	-2.539
ZnAl@LDH	130	10.619	0.038	-0.807	-1.184	-1.561	-1.938
ZnAl@EC	130	-10.766	-0.027	-2.495	-2.123	-1.883	-1.667

adsorption capacity as the number of usage cycles increased. In the first cycle, ZnAl-EC showed the highest adsorption capacity of 76.06 %, followed by ZnAl-LDH and EC. However, with the increase of cycles, all adsorbents experienced a decrease in adsorption capacity. ZnAl-EC, despite its decreasing capacity, remained the best performing adsorbent

until the seventh cycle, where its capacity was still at 33.18 %. On the other hand, adsorbents such as EC experienced the sharpest decline, with the adsorption capacity almost approaching zero from the fifth cycle onwards. These results indicate that although adsorbents such as ZnAl-EC have better regeneration ability, indicating the successful fabrication of adsorption composites the performance after several cycles of use remains, suggesting a limitation in the continuous reuse of adsorbents.

3.6 Adsorption mechanism Study

In this study, the pH optimum adsorption of EC, ZnAl@LDH, and ZnAl@EC adsorbents all have their pH optimum below pH_{pzc}, which indicates adsorption can proceed by chemical adsorption or physical adsorption. Figure 6(a) shows the FTIR characterization of ZnAl@EC before and after adsorption with congo red. Peak 1838 cm^{-1} is identified as the sulfonate group (SO_3^-) of congo red, which shows a sharp peak indicating the successful adsorption of congo red on ZnAl@EC adsorbent, which interacts electrostatically. The peak at 1641 cm^{-1} was identified as hydrogen bonding between the N-H group of Congo red and the surface of ZnAl@EC, which was reinforced by the increasing peak at 3460 cm^{-1} from the hydroxyl group of the adsorbent surface, which hydrogen bonded with the N-H of congo red Ahmad et al. (2023). A schematic illustration of the adsorption mechanism can be seen in Figure 6(b).

4. CONCLUSIONS

The synthesis of ZnAl@EC composites successfully enhanced the adsorption capacity and reusability of ZnAl@LDH for congo red dye removal. The ZnAl@EC composite exhibited the highest adsorption capacity and maintained a considerable amount of its adsorption efficiency after multiple regeneration cycles. The study demonstrates that the incorporation of *Eucheuma cottonii* into ZnAl@LDH not only improves dye adsorption performance but also enhances the material's structural stability and reusability. These findings suggest that ZnAl@EC composites are promising candidates for sustainable and efficient dye removal in wastewater treatment applications.

5. ACKNOWLEDGEMENT

We like to express our gratitude to Hibah Profesi Universitas Sriwijaya according to SK No. 0016/UN9/SK.LP2M.PT/2024 and the Research Center of Inorganic Materials and Coordination Complexes for the support made our research possible.

REFERENCES

Ahmad, N., F. S. Arsyad, I. Royani, P. M. S. B. N. Siregar, T. Taher, and A. Lesbani (2023). High Regeneration of ZnAl/NiAl-Magnetite Humic Acid for Adsorption of Congo Red From Aqueous Solution. *Inorganic Chemistry Communications*, **150**; 110517

Antoniak-Jurak, K., P. Kowalik, W. Próchniak, R. Bicki, and G. Słowik (2021). Heterostructural Mixed Oxides Prepared via ZnAlLa LDH or Ex-ZnAl LDH Precursors-Effect of La Content and Its Incorporation Route. *Materials*, **14**(8); 2082

Basit, A., A. A. Jamali, F. A. Junejo, R. Larik, S. K. Mahar, A. Sameeu, F. K. Mahar, and A. Hyder (2024). Fabrication of CuO Derived Reduced Graphene Oxide Photocatalyst for the Strategic Decolorization of Congo Red From an Aqueous Environment. *Diamond and Related Materials*, **142**; 110839

Cruz, E. D., J. Missau, S. R. Collinson, E. H. Tanabe, and D. A. Bertuol (2023). Efficient Removal of Congo Red Dye Using Activated Lychee Peel Biochar Supported Ca-Cr Layered Double Hydroxide. *Environmental Nanotechnology, Monitoring and Management*, **20**; 100835

Eid, H. A., W. S. Mohamed, A. G. Zaki, S. K. Amer, and E. H. El-Shatoury (2023). Statistical Optimization of Congo Red Biodegradation by a Bacterial Strain of Alcaligenes Faecalis. *Bioresource Technology Reports*, **23**; 101573

Farghali, M. A., A. M. Selim, H. F. Khater, N. Bagato, W. Alharbi, K. H. Alharbi, and I. T. Radwan (2022). Optimized Adsorption and Effective Disposal of Congo Red Dye From Wastewater: Hydrothermal Fabrication of MgAl-LDH Nanohydrotalcite-Like Materials. *Arabian Journal of Chemistry*, **15**(11)

Firdayanti, L., R. Yanti, E. S. Rahayu, and C. Hidayat (2023). Carrageenan Extraction From Red Seaweed (*Kappaphycopsis cottonii*) Using the Bead Mill Method. *Algal Research*, **69**; 102906

Goudjil, S., S. Guergazi, T. Masmoudi, and S. Achour (2021). Effect of Reactional Parameters on the Elimination of Congo Red by the Combination of Coagulation–Floculation With Aluminum Sulfate. *Desalination and Water Treatment*, **209**; 429–436

Han, J. S., S. Y. Kim, and Y. B. Seo (2022). Disk-Shaped Cellulose Fibers From Red Algae, *Eucheuma cottonii* and Its Use for High Oxygen Barrier. *International Journal of Biological Macromolecules*, **210**; 752–758

Haryanto, B., W. B. Singh, E. S. Barus, A. Ridho, and M. R. Rawa (2017). Pseudo Order Kinetics Model to Predict the Adsorption Interaction of Corn-Stalk Adsorbent Surface With Metal Ion Adsorbate Cu (II) and Fe (II). *Journal of Physics: Conference Series*, **801**(1); 012098

Jabeen, A., N. S. Alsaiari, K. M. Katubi, I. Shakir, Z. A. Alrowaili, M. S. Al-Buraihi, and M. F. Warsi (2024). Synthesis and Characterisation of MXene Based-LDH Photocatalytic Materials for the Removal of Toxic Pharmaceutical Effluents. *Journal of Molecular Liquids*, **405**

Jia, Y. H. and Z. H. Liu (2019). Preparation of Borate Anions Intercalated MgAl-LDHs Microsphere and Its Calcinated Product With Superior Adsorption Performance

for Congo Red. *Colloids and Surfaces A: Physicochemical and Engineering Aspects*, **575**; 373–381

Jumaidin, R., S. M. Sapuan, M. Jawaid, M. R. Ishak, and J. Sahari (2017). Characteristics of *Eucheuma cottonii* Waste From East Malaysia: Physical, Thermal and Chemical Composition. *European Journal of Phycology*, **52**(2); 200–207

Kang, J., M. Liu, M. Qu, X. Guang, J. Chen, Y. Zhao, and B. Huang (2023). Identifying the Potential Soil Pollution Areas Derived From the Metal Mining Industry in China Using MaxEnt With Mine Reserve Scales (MaxEnt_MRS). *Environmental Pollution*, **329**; 121687

Lesbani, A., N. Ahmad, R. Mohadi, I. Royani, S. Wibiyan, Amri, and Y. Hanifah (2024). Selective Adsorption of Cationic Dyes by Layered Double Hydroxide With Assist Algae (Spirulina Platensis) to Enrich Functional Groups. *JCIS Open*, **15**

Li, Z., J. Wang, D. F. Expósito, J. Zhang, C. Fu, D. Shi, and D. Y. Wang (2018). High-Performance Carrageenan Film Based on Carrageenan Intercalated Layered Double Hydroxide With Enhanced Properties: Fire Safety, Thermal Stability and Barrier Effect. *Composites Communications*, **9**; 1–5

Majid, N. B., I. S. B. Ibrahim, N. N. B. Sarbini, Z. A. B. Zakaria, and M. H. B. Osman (2019). The Chemical Properties of Seaweed for Modify Concrete. *IOP Conference Series: Earth and Environmental Science*, **220**(1); 012026

Meili, L., P. V. Lins, C. L. P. S. Zanta, J. I. Soletti, L. M. O. Ribeiro, C. B. Dornelas, T. L. Silva, and M. G. A. Vieira (2019). MgAl-LDH/Biochar Composites for Methylene Blue Removal by Adsorption. *Applied Clay Science*, **168**; 11–20

Nissa, R. C., A. H. D. Abdullah, B. Firdiana, W. Kosasih, E. S. Endah, S. Marliah, A. Rahmat, and Hidayat (2023). Characterization of Microcrystalline Cellulose From Red Seaweed *Gracilaria Verucosa* and *Eucheuma cottonii*. *IOP Conference Series: Earth and Environmental Science*, **1201**(1); 012101

Noli, F., M. Sidirelli, and P. Tsamos (2024). The Impact of Phosphate Fertilizer Factory on the Chemical and Radiological Pollution of the Surrounding Marine Area (Seawater and Sediments) in Northwestern Greece. *Regional Studies in Marine Science*, **73**

Ravichandran, K., N. S. Jyothi, K. Thirumurugan, S. Suvathi, N. Chidhambaram, R. Uma, and B. Sundaresan (2023). Influence of Mo + F Incorporation and Point of Zero Charge on the Dye Degradation Efficacy of ZnO Thin Films. *Chemical Physics*, **564**

Rohmatullaili, N. Ahmad, D. Savira, D. Erviana, Zultriana, R. Mohadi, and A. Lesbani (2024). A Series of MgAl Layer Double Hydroxide-Based Materials Intercalated With Clitoria Ternatea Flower Extract as Photocatalysts in the Ciprofloxacin Degradation. *Chemical Physics Impact*, **8**

Sahu, A. and J. C. Poler (2024). Removal and Degradation of Dyes From Textile Industry Wastewater: Benchmarking Recent Advancements, Toxicity Assessment and Cost Analysis of Treatment Processes. *Journal of Environmental Chemical Engineering*, **12**(5)

Shen, J., A. Shi, M. Wu, H. Zhang, and Z. Jiang (2022). Efficient Degradation of Bisphenol A Over Facilely Optimized Ternary Ag/ZnO/ZnAl-LDH Composite With Enhanced Photocatalytic Performance Under Visible Light Irradiation. *Solid State Sciences*, **132**

Silva, C. E. d. F., B. M. V. d. Gama, A. H. d. S. Gonçalves, J. A. Medeiros, and A. K. d. S. Abud (2020). Basic-Dye Adsorption in Albedo Residue: Effect of pH, Contact Time, Temperature, Dye Concentration, Biomass Dosage, Rotation and Ionic Strength. *Journal of King Saud University - Engineering Sciences*, **32**(6); 351–359

Taher, T., R. Putra, N. R. Palapa, and A. Lesbani (2021). Preparation of Magnetite-Nanoparticle-Decorated NiFe Layered Double Hydroxide and Its Adsorption Performance for Congo Red Dye Removal. *Chemical Physics Letters*, **777**

Tang, L., W. Chen, F. Li, J. Xu, Y. Shi, and H. Jiang (2024). The Formation and Adsorption Mechanism Studies of 3D Hydrangea-Like ZnFe-LDHs/FeOOH for the Highly Efficient Removal of Phosphate. *Chemical Engineering Journal*, **482**

Tye, Y. Y., A. H. Khalil, C. Y. Kok, and C. K. Saurabh (2018). Preparation and Characterization of Modified and Unmodified Carrageenan Based Films. *IOP Conference Series: Materials Science and Engineering*, **368**(1)

Umesh, A. S., Y. M. Puttaiahgowda, and S. Thottathil (2024). Enhanced Adsorption: Reviewing the Potential of Reinforcing Polymers and Hydrogels With Nanomaterials for Methylene Blue Dye Removal. *Surfaces and Interfaces*, **51**; 104670

Wulandari, D., Y. Kilawati, and M. Fadjar (2018). Activity of Compounds on Seaweed *Eucheuma cottonii* Extract as Antioxidant Candidate to Prevent Effects of Free Radical in Water Pollution. *Research Journal of Life Science*, **5**(3); 173–182

Yao, C., Y. Yang, C. Li, Z. Shen, J. Li, N. Mei, C. Luo, Y. Wang, C. Zhang, and D. Wang (2024). Heavy Metal Pollution in Agricultural Soils from Surrounding Industries with Low Emissions: Assessing Contamination Levels and Sources. *Science of the Total Environment*, **917**; 170610

Yuliarti, O., A. D. Sentana, C. Y. Ong, Z. Abdol Rahim Yassin, L. Ng, and W. M. Koh (2023). Structural Properties of *cottonii* Seaweed (*Kappaphycus alvarezii*) Gels in the Presence of Coconut Milk. *Food Hydrocolloids*, **145**; 109087

Zhang, X., W. Li, X. Wang, M. Su, and Q. Lin (2024). A Novel 3D Hierarchical NiFe-LDH/Graphitic Porous Carbon Composite as Multifunctional Adsorbent for Efficient Removal of Cationic/Anionic Dyes and Heavy Metal Ions. *Journal of Molecular Liquids*, **411**; 125753

Zhu, S., M. A. Khan, T. Kameda, H. Xu, F. Wang, M. Xia,

and T. Yoshioka (2022). New Insights into the Capture Performance and Mechanism of Hazardous Metals Cr3+ and Cd2+ onto an Effective Layered Double Hydroxide Based Material. *Journal of Hazardous Materials*, **426**; 128062

Zong, P., S. Wang, G. Liang, M. Shao, N. Yan, X. Xu, M. Xu, W. Li, Y. Yang, J. Chen, and Z. Qiu (2022). Eco-Friendly Approach for Effective Removal for Congo Red Dye from Wastewater Using Reusable Zn-Al Layered Double Hydroxide Anchored on Multiwalled Carbon Nanotubes Supported Sodium Dodecyl Sulfonate Composites. *Journal of Molecular Liquids*, **349**; 118468

